NASA TECHNICAL NOTE

NASA TN D-4978

C.1

NASA TN D-4978

BACK FLOW FROM JET PLUMES IN VACUUM

by Norman T. Grier

Lewis Research Center
Cleveland, Ohio

NATIONAL AERONAUTICS AND SPACE ADMINISTRATION • WASHINGTON, D. C. • JANUARY 1969

BACK FLOW FROM JET PLUMES IN VACUUM

By Norman T. Grier

Lewis Research Center
Cleveland, Ohio

NATIONAL AERONAUTICS AND SPACE ADMINISTRATION

For sale by the Clearinghouse for Federal Scientific and Technical Information
Springfield, Virginia 22151 – CFSTI price $3.00

ABSTRACT

Approximate calculations were performed to determine the increase in particle density at points surrounding a jet nozzle due to the exhausted gas in the jet plume. The calculations were made for helium, argon, and nitrogen for a nozzle throat radius of 1 centimeter. The chamber density ranged from 10^{-8} to 1 gram per cubic centimeter. The plume flow is assumed radial with the source point at the nozzle exit on the nozzle axis.

BACK FLOW FROM JET PLUMES IN VACUUM

by Norman T. Grier

Lewis Research Center

SUMMARY

Approximate calculations were performed to determine the increase in particle density at points surrounding a jet nozzle due to the exhausted gas in the jet plume. The calculations were made for nitrogen, helium, and argon for a nozzle throat radius of 1 centimeter. The chamber density ranged from 10^{-8} to 1 gram per cubic centimeter. The plume flow is assumed radial with the source point at the nozzle exit on the nozzle axis. The results indicate that for a chamber density of 1 gram per cubic centimeter, the back flow density could be as high as 10^6 to 10^7 particles per cubic centimeter.

INTRODUCTION

For spacecraft accelerating or maneuvering in space, the back flow from the jet exhaust may be a large contributor to the ambient environment of the spaceship. If this exhaust gas is detrimental in any manner to the planned purpose of the flight, special shielding may be required. In order to get an estimate of the density of the back flow, an approximate calculation is performed in this report. The gases used are helium, nitrogen, and argon. In all the calculations the jet exit Mach number M_e is 5.

The results presented in this report may be considered an extension of a companion paper published in the Proceedings of the Sixth International Symposium on Rarefied Gasdynamics (ref. 1). In that paper, results for points located up to 100 exit radii in the plane of the nozzle exit are presented. In this report, results are presented for points located up to 1000 exit radii in the plane of the nozzle exit as well as for points in planes ahead of the nozzle exit. Also, in the previous paper (ref. 1), the maximum angle that the plume flow could turn through was assumed to be the Prandtl-Meyer expansion angle. This assumption is not made herein. Rather it is assumed that the analysis of Hill and Draper (ref. 2) is valid throughout the plume flow field. And finally, the analysis presented herein is more detailed than that of the previous paper (ref. 1).

The gas in the plume is considered to be continuum until the density is such that the mean free path is comparable to the distance the particular mass of gas has travelled from the nozzle exit. That is, the jet flow is continuum until the Knudsen number has a value near one. Afterwards, the flow is assumed free molecular with no interparticle collisions occurring. This model is shown in figure 1.

Since most of the constant Knudsen surface is usually far from the jet exit plane, it is assumed that the flow has nearly reached its adiabatic limit and has a radial direction, that is, the streamlines diverge from a common source point located at the nozzle exit. The validity of these assumptions is discussed in references 2, 3, and 4. The calculations were performed for a nozzle throat radius of 1 centimeter, a value of Knudsen number of one, and chamber densities ranging from 10^{-8} to 1 gram per centimeter. For a chamber temperature of 300 K, these densities correspond to chamber pressures for helium of $\sim 6\times10^{-5}$ to 6×10^{3} atmospheres, for argon of $\sim 6\times10^{-6}$ to 6×10^{2} atmospheres, and for nitrogen of $\sim 9\times10^{-6}$ to $\sim 9\times10^{2}$ atmospheres. In all the calculations the environment excluding the exhaust gas was assumed to be a total vacuum. A high-speed digital computer was used for the calculation.

ANALYSIS

As mentioned earlier, references 2, 3, and 4 show that far from the nozzle exit, the exhaust from jet nozzles in vacuum can be closely approximated by radial flow. For radial flow, the mass flux ρV varies inversely as the square of the distance from the source point. Far from the source, the flow has nearly attained its adiabatic velocity limit, so the density decrease along each streamline is proportional to the inverse square of the distance from the source. Applying this description to jet plumes, references 2, 3, and 4 show that the density along the plume axis ($\theta = 0$) is approximately given by

$$\rho_{\theta=0} = 4\rho_c B\left(\frac{r^*}{r}\right)^2 \qquad (1)$$

where r^* is the nozzle throat radius, r is the distance from the source point which is assumed located on the nozzle axis in the plane of the nozzle exit, ρ_c is the chamber density, and B is a constant that depends on the type of gas. (See fig. 2 for coordinate system.) (All symbols are defined in the appendix.) For r constant the density may be written approximately as a function of θ as (ref. 2)

$$\rho = \rho_{\theta=0} e^{-\lambda^2(1-\cos\theta)^2}$$

$$= 4\rho_c B\left(\frac{A^*}{A_e}\right)\left(\frac{r_e}{r}\right)^2 e^{-\lambda^2(1-\cos\theta)^2} \tag{2}$$

where r_e is the nozzle exit radius

$$\lambda = \frac{1}{\sqrt{\pi}\left(1 - \frac{C_F}{CC_{F_{max}}}\right)} \tag{3}$$

$$B = \frac{\lambda}{4C\sqrt{\pi}}\left(\frac{\gamma - 1}{\gamma + 1}\right)^{1/2}\left(\frac{2}{\gamma + 1}\right)^{1/(\gamma-1)} \tag{4}$$

where C_F is the thrust coefficient and C is the ratio of the velocity to the maximum velocity. The ratio, C, is assumed to be approximately 1 on the constant Knudsen surface. The thrust coefficient C_F was evaluated using equation (4.33) of reference 5.

Equations (1) to (4) apply as long as the flow is continuum. Actually a transition from continuum to free molecular flow occurs over a region in the plume. It is assumed, however, that this region can be approximated by a surface on which the Knudsen number is constant. For the present study, the Knudsen number is defined by

$$K = \frac{l}{r} \tag{5}$$

where l is the mean free path and is given in reference 6 approximately as

$$l = 3.736\times10^{-25}\,\frac{M}{\rho\delta^2}, \qquad \text{cm} \tag{6}$$

where M is the molecular weight in gram per gram-mole and δ is the molecular diameter of the molecules in centimeters. Substituting equation (6) into equation (5) and solving for ρ yield

$$\rho = 3.736\times10^{-25} \frac{M}{K\delta^2 r_e\left(\frac{r}{r_e}\right)} \tag{7}$$

Equating equations (7) and (2) results in the following equation of the constant Knudsen surface

$$\frac{r}{r_e} = 1.07\times10^{25} \frac{K\rho_c r^{*}\delta^2 B}{M}\left(\frac{A^*}{A_e}\right)^{1/2} e^{-\lambda^2(1-\cos\theta)^2} \tag{8}$$

In equation (8) the maximum value for θ was taken as the value corresponding to a value of r/r_e of 0.1. Solving equation (8) for θ_{max} gives

$$\theta_{max} = \arc\cos\left\{1 - \frac{1}{\lambda}\sqrt{\ln\left[1.07\times10^{24} \frac{BK\delta^2\rho_c r_e}{M}\left(\frac{A^*}{A_e}\right)\right]}\right\} \tag{9}$$

To determine the effect of limiting r/r_e to values greater than 0.1, a calculation was made using a θ_{max} corresponding to r/r_e of 0.05. The difference could not be discerned on the figures. Where there was any difference, it occurred for y/r_e less than 20.

On the constant Knudsen surface, the gas is assumed Maxwellian with a mean velocity $\vec{V}$ in the radial direction. From Nöller's report (ref. 7), the density at a point P(x, y, z) due to the molecules leaving the elemental volume $d\tau$ adjacent to the constant Knudsen surface is

$$dn_P = n_\tau \pi^{-3/2} e^{-U^2}\left\{\frac{1}{2} U \cos\psi + \left(\frac{1}{2} + U^2\cos^2\psi\right) e^{U^2\cos^2\psi}\left(\frac{\sqrt{\pi}}{2}\right)\left[1 + \mathrm{erf}(U\cos\psi)\right]\right\} d\Omega \tag{10}$$

where n_τ is the number density of molecules in $d\tau$, $U = |V|/(2RT/M)^{1/2}$, that is $|\vec{V}|$ nondimensionalized with respect to the most probable thermal velocity, ψ is the angle between the direction of $\vec{V}$ and the direction of flight of the molecules contributing to the density at P(x, y, z), erf $(U \cos \psi)$ is the error function, and $d\Omega$ is the element of solid angle of $d\tau$ as seen from point P(x, y, z).

Using the coordinate system shown in figure 1 gives

$$\cos \psi = \vec{L} \cdot \frac{\hat{r}}{|\vec{L}|} \tag{11}$$

$$d\Omega = \frac{\vec{L} \cdot \hat{n}\, d\sigma}{|\vec{L}|^3} \tag{12}$$

where $\vec{L}$ is the vector from $d\tau$ to the point $P(x,y,z)$, $\hat{r}$ is the unit vector in the radial direction, $\hat{n}$ is the unit vector normal to the constant Knudsen surface at $d\tau$, and $d\sigma$ is an element of area on the constant Knudsen surface at $d\tau$. The coordinates for $d\tau$ are denoted by (r, θ, φ) and the coordinates for point P by (x,y,z). Using figure 2 and restricting x to be zero (the plume is symmetrical about the z-axis) result in

$$\frac{\vec{L}}{r_e} = \hat{r}\left(\frac{y}{r_e} \sin\theta \cos\varphi - \frac{r}{r_e} + \frac{z}{r_e} \cos\theta\right) + \hat{\theta}\left(\frac{y}{r_e} \cos\theta \cos\varphi - \frac{z}{r_e} \sin\theta\right) - \hat{\varphi}\, \frac{y}{r_e} \sin\varphi \tag{13}$$

where $\hat{r}$, $\hat{\theta}$, and $\hat{\varphi}$ are the spherical coordinate unit vectors. Substituting equation (13) in equation (11) yields

$$\cos\psi = \frac{\frac{y}{r_e} \sin\theta \cos\varphi - \frac{r}{r_e} + \frac{z}{r_e} \cos\theta}{\left|\frac{\vec{L}}{r_e}\right|} \tag{14}$$

Now on the constant Knudsen surface, r is related to θ through equation (8), which can be written as

$$r = r_{\theta=0}\, e^{-\lambda^2(1-\cos\theta)^2} \tag{15}$$

where

$$r_{\theta=0} = 1.07\times10^{25}\, \frac{B\rho_c r^* K\delta^2}{M}\left(\frac{A^*}{A_e}\right) r_e \tag{16}$$

Equations (15) and (16) define the constant Knudsen surface in terms of θ as an independent variable. The other independent variable is the azimuthal angle φ. Therefore, (ref. 8)

$$\hat{n}\, d\sigma = \frac{\partial \vec{r}}{\partial \theta} \times \frac{\partial \vec{r}}{\partial \varphi}\, d\theta\, d\varphi \tag{17}$$

Now

$$\vec{r} = \hat{r} r_{\theta=0}\, e^{-\lambda^2 (1-\cos\theta)^2} \tag{18}$$

So that

$$\frac{\partial \vec{r}}{\partial \theta} = r_{\theta=0} e^{-\lambda^2 (1-\cos\theta)^2} \left[-\hat{r} 2\lambda^2 (1 - \cos\theta) \sin\theta + \hat{\theta}\right] \tag{19}$$

$$\frac{\partial \vec{r}}{\partial \varphi} = r \frac{\partial \hat{r}}{\partial \varphi} = \hat{\varphi} r \sin\theta \tag{20}$$

Therefore,

$$\hat{n}\, d\sigma = \left[\hat{\theta} 2\lambda^2 (1 - \cos\theta) \sin\theta + \hat{r}\right] r^2 \sin\theta\, d\theta\, d\varphi \tag{21}$$

Substituting equations (13) and (21) into equation (12) gives

$$d\Omega = \left[\frac{y}{r_e} \sin\theta \cos\varphi \left(1 + 2\lambda^2 \cos\theta - 2\lambda^2 \cos^2\theta\right)\right] - \frac{r}{r_e}$$

$$+ \frac{z}{r_e}\left(\cos\theta - 2\lambda^2 \sin^2\theta + 2\lambda^2 \sin^2\theta \cos\theta\right)\left(\frac{r}{r_e}\right)^2 \left(\frac{r_e}{L}\right)^3 \sin\theta\, d\theta\, d\varphi \tag{22}$$

The density at point $P(0, y, z)$ due to molecules leaving the total surface is

$$n_P = \pi^{-3/2} e^{-U^2} \int_{\theta=0}^{\theta=\theta_{max}} \int_{\varphi=-\pi/2}^{\varphi=\pi/2} d\Omega\, n_\tau \left\{ \frac{1}{2} U \cos\psi + \left(\frac{1}{2} + U^2\cos^2\psi\right) e^{U^2\cos^2\psi} \left(\frac{\sqrt{\pi}}{2}\right) \left[1 + \mathrm{erf}(U\cos\psi)\right] \right\} \tag{23}$$

where θ_{max} is given by equation (9), $d\Omega$ is given by equation (22), and $\cos\psi$ is given by equation (14).

In order to get the results presented, it was assumed that the velocity V was 95 percent of its adiabatic limiting velocity. This precludes the necessity of assuming a value for the temperature. The gas is assumed to be ideal. Therefore, the equation for the dimensionless velocity U is

$$U = \frac{V}{V_{max}} \sqrt{\frac{\gamma}{(\gamma - 1)\left(1 - \frac{V^2}{V_{max}^2}\right)}}$$

$$= 0.95 \sqrt{\frac{\gamma}{0.0975(\gamma - 1)}}$$

The molecular diameter δ required for the various gases are (ref. 6) as follows:

Nitrogen:	3.76×10^{-8} cm
Helium:	2.18×10^{-8} cm
Argon:	3.67×10^{-8} cm

The number density n_τ is

$$n_\tau = \frac{N_o}{M} \rho_\tau$$

where N_o is Avogadro's number and ρ_τ is given by equation (2) or (7) evaluated at $d\tau$.

RESULTS AND DISCUSSION

A typical shape of the constant Knudsen surface is shown in figure 1. This figure is drawn to scale relative to the exit radius shown for helium using $K = 1$, $r^* = 1$ centimeter, and $\rho_c = 10^{-7}$ gram per cubic centimeter. This Knudsen surface extends to approximately 34 r_e. If the chamber density had been 1 gram per cubic centimeter, the surface would be 10^7 times larger. This follows from equation (16) where it can be seen that $r_{\theta=0}$ varies linearly with the chamber density.

In figures 3 to 5 is shown the back flow number density for helium, argon, and nitrogen, respectively, for values of y/r_e up to 1000. The results are given for chamber densities from 10^{-8} to 1 gram per cubic centimeter, a Knudsen number of 1, and a nozzle throat radius of 1 centimeter. Because of approximations made in the analysis, the results are only expected to indicate trends and to give an order of magnitude of the back flow density. The results for helium and argon show the effect of changing the molecular weight by a factor of 10. From figures 3 and 4 it is seen that in no case does the back flow density decrease by a factor of ten. In most cases the decrease in changing from helium to argon is only by a factor of approximately four.

The calculation for nitrogen shows the effect of changing from a monatomic to a diatomic gas. Comparing figures 3 and 4 with figure 5 shows that the back flow for nitrogen decreases much faster with y/r_e than does helium or argon. Also it is noticed that the back flow density for nitrogen also decreases faster with chamber density than it does for helium or argon. As was indicated previously, the difference in molecular weights cannot account for this variation. So most of the difference in the behavior of nitrogen from that of helium and argon must be due to the difference in the value of γ. This causes λ and U to be different.

One final point to be noticed from the figures is that the back flow in the plane of the nozzle exit continues to decrease as the distance from the nozzle y/r_e increases. The back flow for points located in planes ahead of the nozzle exit, however, first increases, peaks, then decreases as y/r_e increases. This can be seen from figures 3 to 5. The peaks are broadest for planes located the farthest from the nozzle exit. The calculations were made for planes located 0, 2, 5, and 10 exit radii ahead of the nozzle exit.

Lewis Research Center,
National Aeronautics and Space Administration,
Cleveland, Ohio, October 23, 1968,
124-09-19-01-22.

APPENDIX - SYMBOLS

A^* nozzle throat area, cm^2

A_e nozzle exit area, cm^2

B defined by eq. (4), dimensionless

C ratio of velocity to maximum velocity

C_F nozzle thrust coefficient

$C_{F_{max}}$ maximum nozzle thrust coefficient

K Knudsen number, l/r

$\vec{L}$ vector distance from $d\tau$ on constant Knudsen surface to point $P(x,y,z)$, cm

l mean free path of gas particles, cm

M molecular weight of gas

M_e nozzle exit Mach number

N_o Avogadro's number, particles/g-mole

n particle density, particles/cm^3

$\hat{n}$ unit vector normal to constant Knudsen surface

n_p particle density at point $P(x,y,z)$, particles/cm^3

n_τ particle density in volume element $d\tau$

R gas constant

r^* nozzle throat radius, cm

r_e nozzle exit radius

r, θ, φ spherical coordinates

$\hat{r}, \hat{\theta}, \hat{\varphi}$ unit vectors of r, θ, φ

U dimensionless velocity, $|\vec{V}| / (2RT/M)^{1/2}$

$\vec{V}$ mean velocity of particles in jet, cm/sec

γ isentropic exponent

δ molecular diameter of molecule, cm

λ defined by eq. (3)

ρ mass density, g/cm^3

ρ_c chamber mass density, g/cm^3

ψ angle between direction of $\vec{V}$ and direction of $\vec{L}$

REFERENCES

1. Grier, Norman T.: Back Flow from Jet Plumes in Vacuum. Presented at the 6th Rarefied Gas Dynamics Symposium, Cambridge, Mass., July 22-26, 1968.

2. Hill, Jacques A. F.; and Draper, James Stark: Analytical Approximation for the Flow from a Nozzle into a Vacuum. J. Spacecraft and Rockets, vol. 3, no. 10, Oct. 1966, pp. 1552-1554.

3. Sherman, F. S.: Self-Similar Development of Inviscid Hypersonic Free-Jet Flows. Rep. 6-90-63-61, Lockheed Missiles and Space Co., May 23, 1963. (Available from DDC as AD-618954).

4. Albini, Frank A.: Approximate Computation of Underexpanded Jet Structure. AIAA J., vol. 3, no. 8, Aug. 1965, pp. 1535-1537.

5. Shapiro, Ascher H.: The Dynamics and Thermodynamics of Compressible Fluid Flow. Vol. 1. The Ronald Press Co., 1953.

6. Santeler, Donald J.; Holkeboer, David H.; Jones, Donald W.; and Pagano, Frank: Vacuum Technology and Space Simulation. NASA SP-105, 1966.

7. Nöller, H. G.: Approximate Calculation of Expansion of Gas from Nozzles into High Vacuum. J. Vacuum Sci. Tech., vol. 3, no. 4, July/Aug. 1966, pp. 202-207.

8. Phillips, H. B.: Vector Analysis. John Wiley & Sons, Inc., 1933.

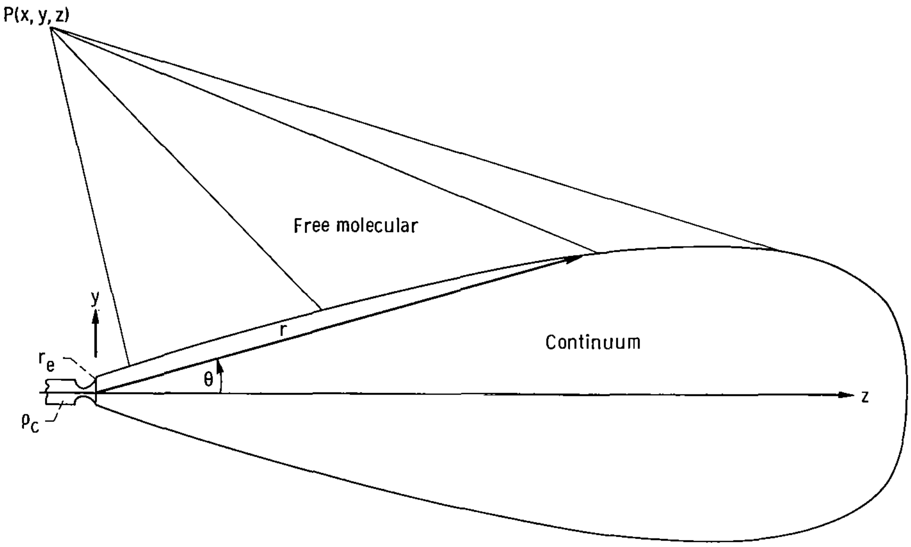

Figure 1. - Representative constant Knudsen surface shown to scale for helium for Knudsen number K = 1, nozzle throat radius $r^* = 1$ centimeter, and chamber density ρ_c of 10^{-7} gram per cubic centimeter.

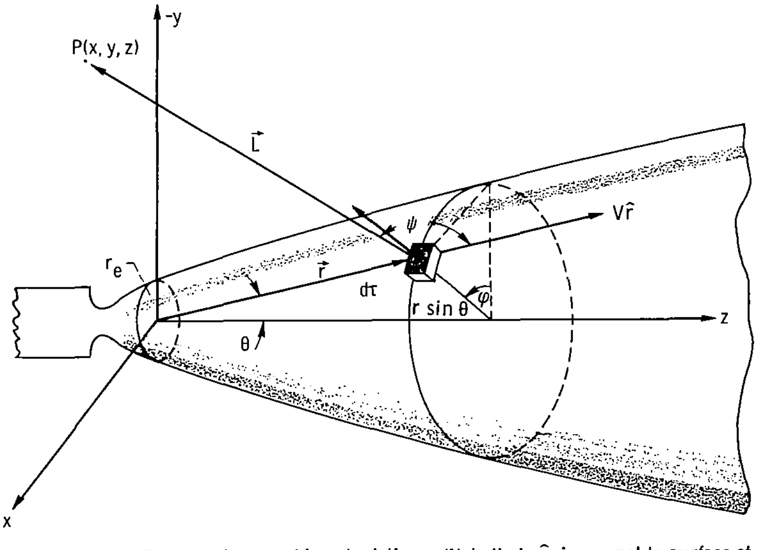

Figure 2. - Coordinate system used in calculations. (Note that $\hat{n}$ is normal to surface at dτ and $\hat{r} = \vec{r}/|r|$.)

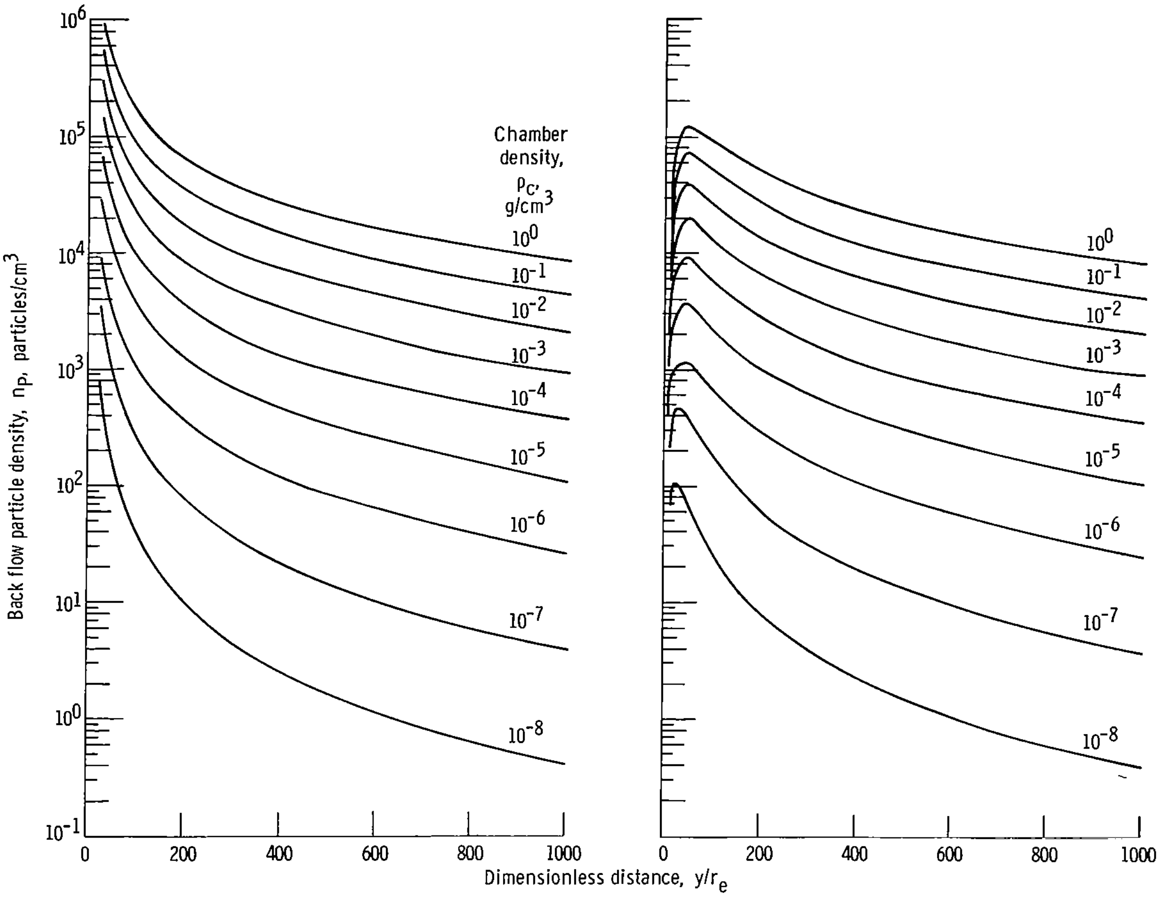

(a) For points in plane of nozzle exit (i.e., $z/r_e = 0$).

(b) For points located in plane $2r_e$ ahead of nozzle exit (i.e., $z/r_e = -2$).

Figure 3. - Helium back flow density plotted against distance from nozzle axis for Knudsen number $K = 1$ and nozzle throat radius $r^* = 1$ centimeter.

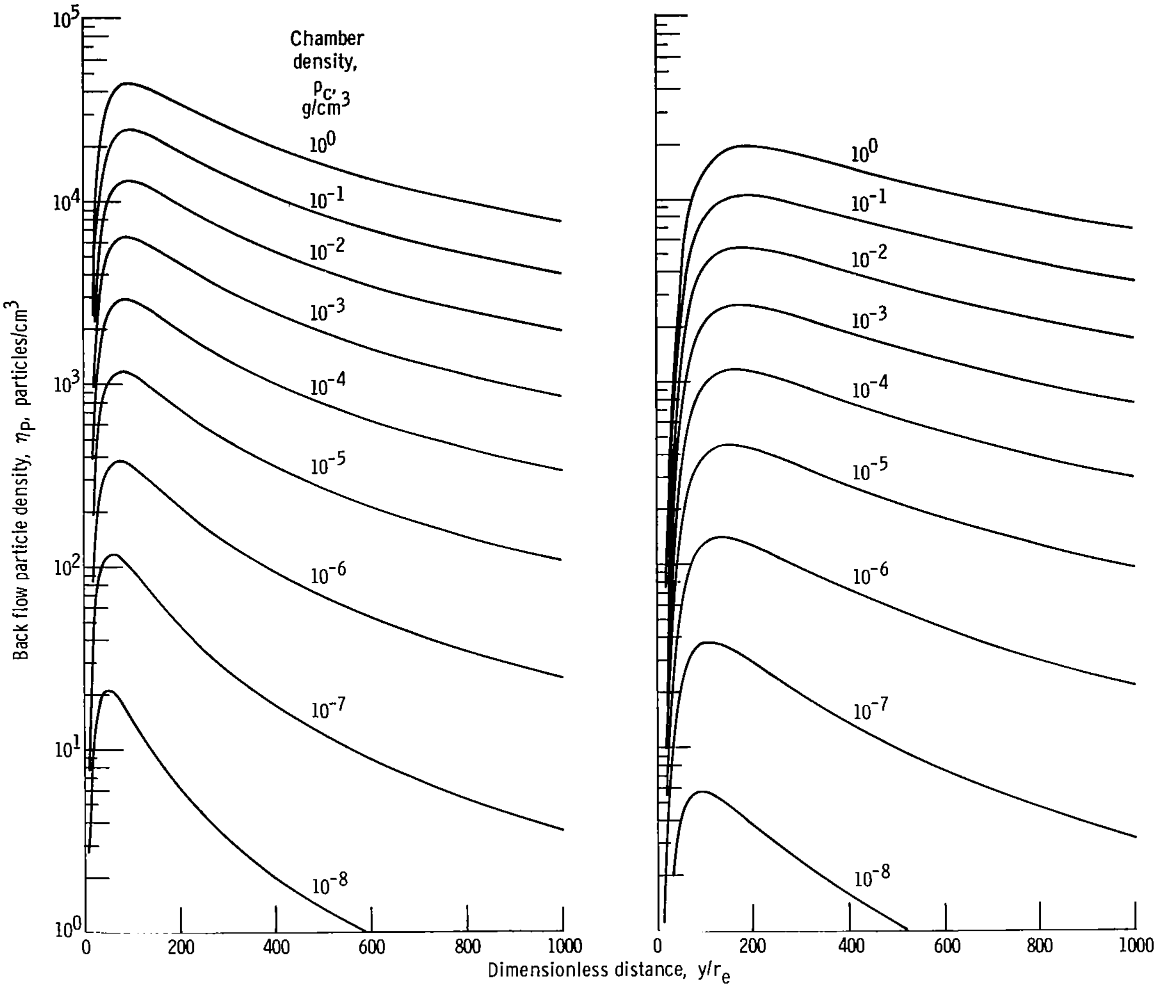

(c) For points located in plane $5r_e$ ahead of nozzle exit (i.e., $z/r_e = -5$).

(d) For points located in plane $10r_e$ ahead of nozzle exit (i.e., $z/r_e = -10$).

Figure 3. - Concluded.

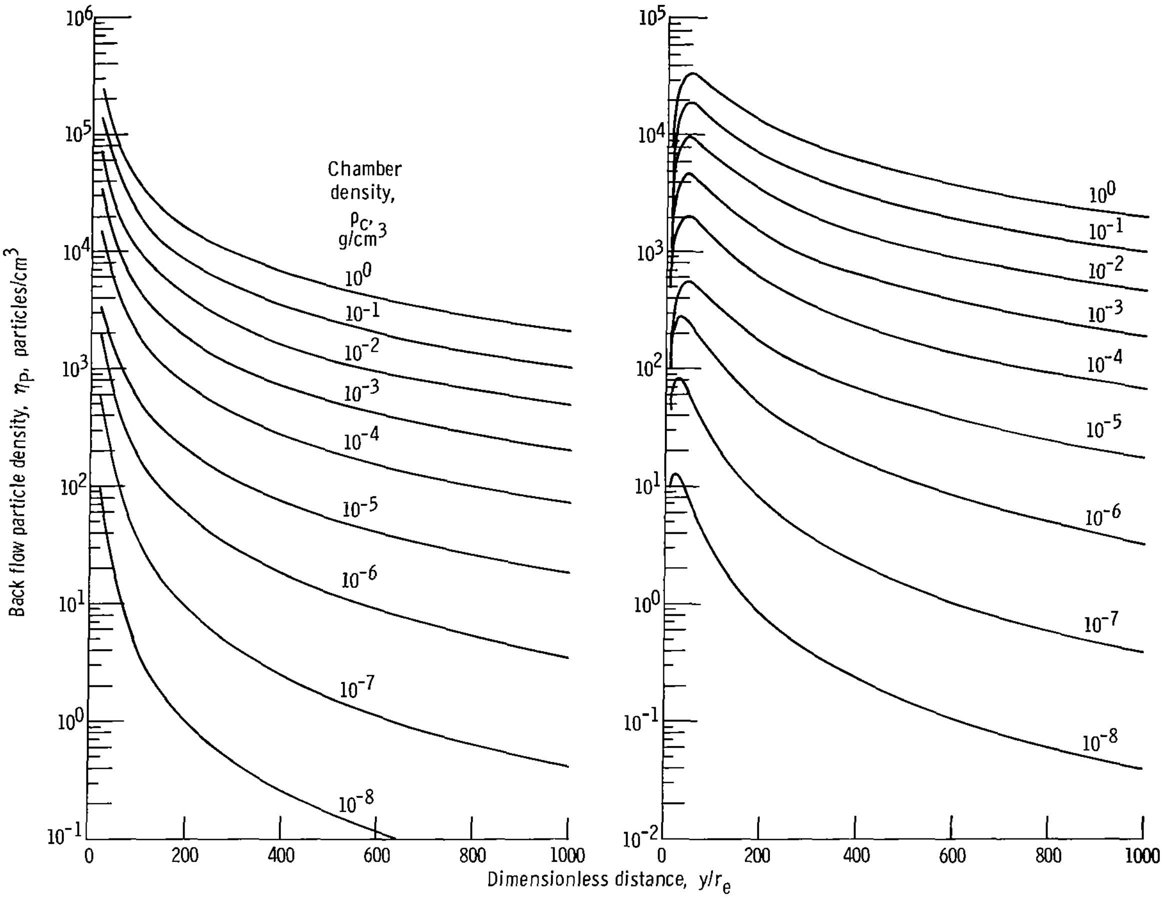

(a) For points in plane of nozzle exit (i.e., $z/r_e = 0$).

(b) For points located in plane $2r_e$ ahead of nozzle exit (i.e., $z/r_e = -2$).

Figure 4. - Argon back flow density plotted against distance from nozzle axis for Knudsen number K = 1 and nozzle throat radius $r^* = 1$ centimeter.

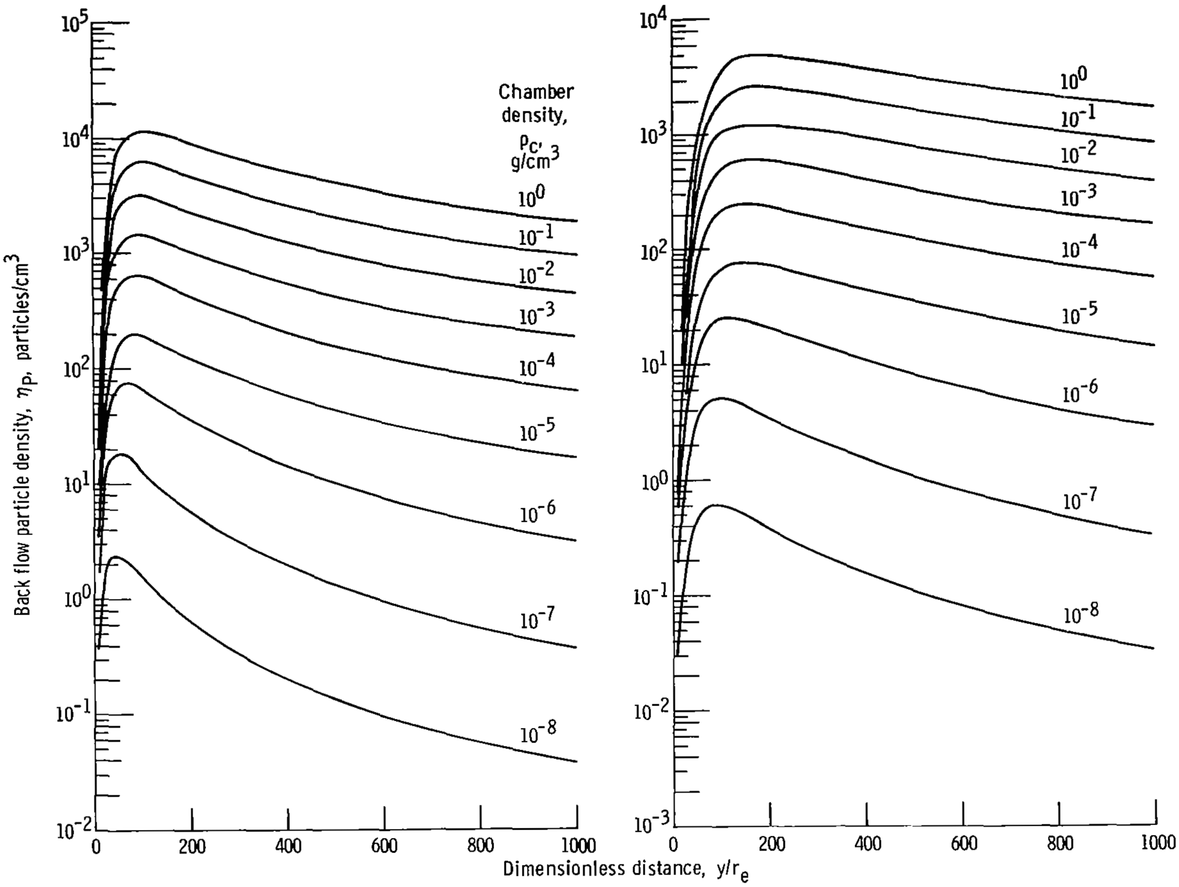

(c) For points located in plane $5r_e$ ahead of nozzle exit (i.e., $z/r_e = -5$).

(d) For points located in plane $10r_e$ ahead of nozzle exit (i.e., $z/r_e = -10$).

Figure 4. - Concluded.

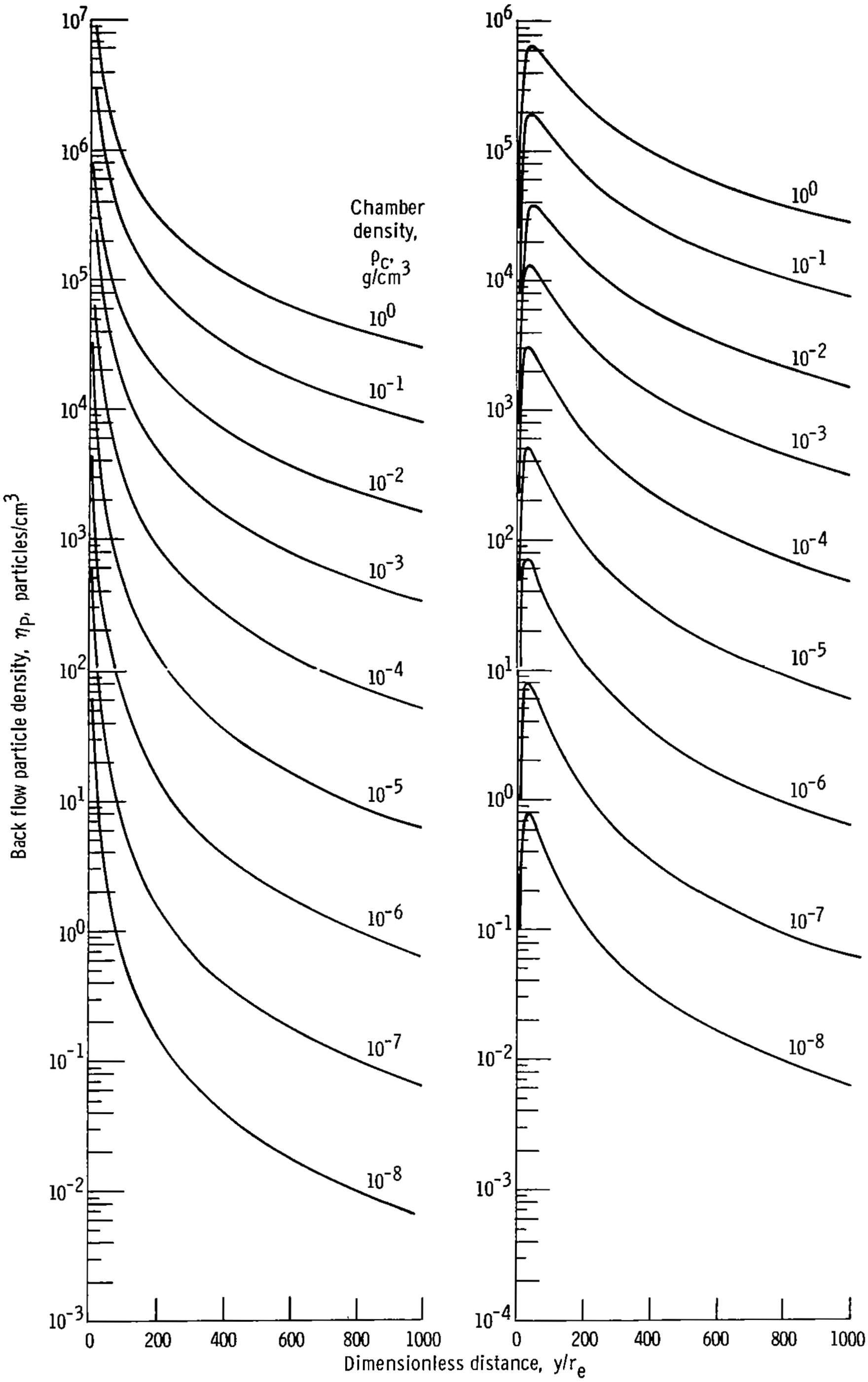

(a) For points in plane of nozzle exit (i.e., $z/r_e = 0$).

(b) For points located in plane $2r_e$ ahead of nozzle exit (i.e., $z/r_e = -2$).

Figure 5. - Nitrogen back flow density plotted against distance from nozzle axis for Knudsen number $K = 1$ and nozzle throat radius $r^* = 1$ centimeter.

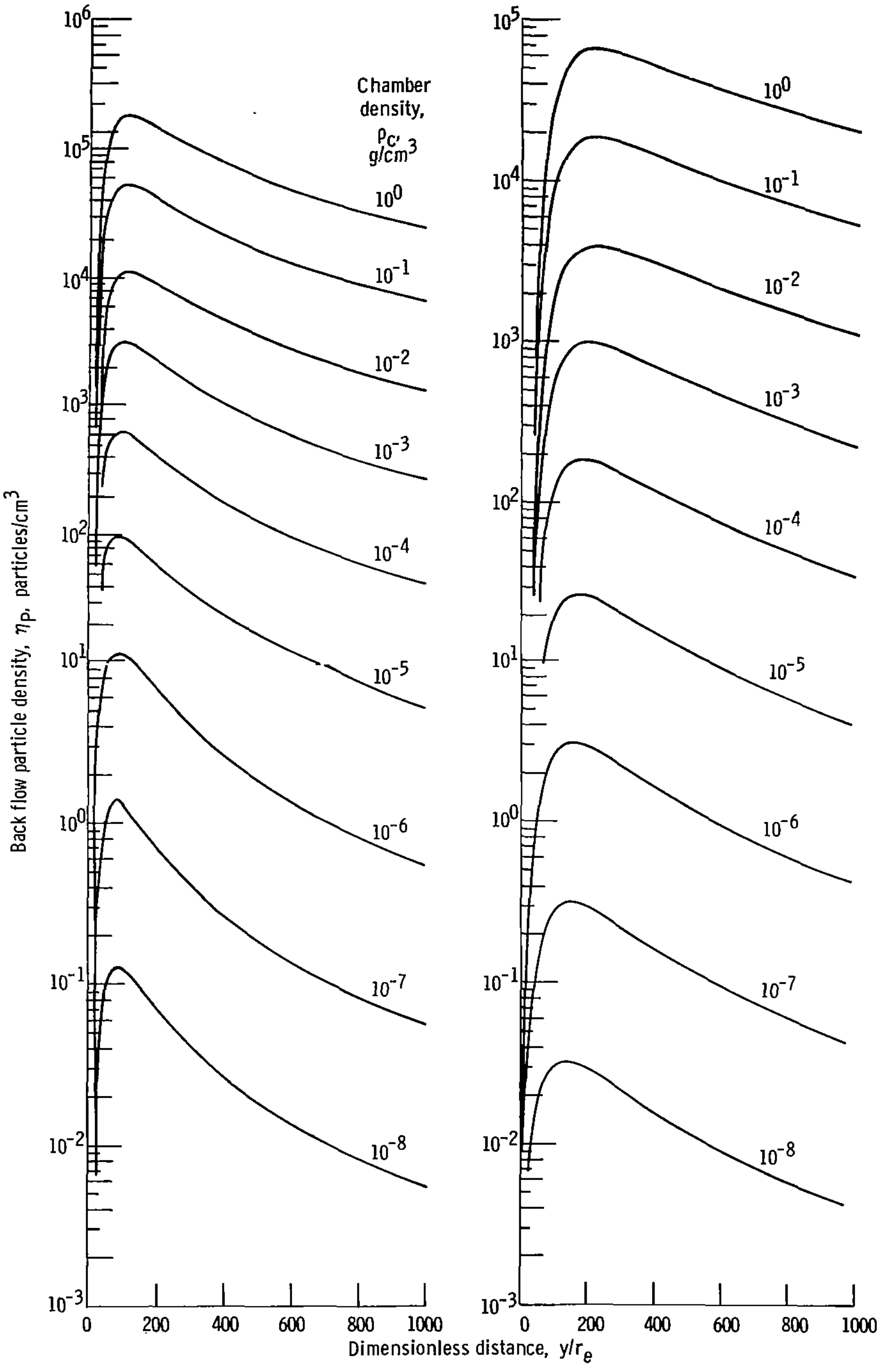

(c) For points located in plane $5r_e$ ahead of nozzle exit (i.e., $z/r_e = -5$).

(d) For points located in plane $10r_e$ ahead of nozzle exit (i.e., $z/r_e = -10$).

Figure 5. - Concluded.